

LETTERS

Photon-by-photon feedback control of a single-atom trajectory

A. Kubanek¹, M. Koch¹, C. Sames¹, A. Ourjoutsev¹, P. W. H. Pinkse¹, K. Murr¹ & G. Rempe¹

Feedback is one of the most powerful techniques for the control of classical systems. An extension into the quantum domain is desirable as it could allow the production of non-trivial quantum states^{1–4} and protection against decoherence^{5,6}. The difficulties associated with quantum, as opposed to classical, feedback arise from the quantum measurement process—in particular the quantum projection noise and the limited measurement rate—as well as from quantum fluctuations perturbing the evolution in a driven open system. Here we demonstrate real-time feedback control^{7–12} of the motion of a single atom trapped in an optical cavity. Individual probe photons carrying information about the atomic position^{13,14} activate a dipole laser that steers the atom on timescales 70 times shorter than the atom's oscillation period in the trap. Depending on the specific implementation, the trapping time is increased by a factor of more than four owing to feedback cooling, which can remove almost all the kinetic energy of the atom in a quarter of an oscillation period¹². Our results show that the detected photon flux reflects the atomic motion, and thus mark a step towards the exploration of the quantum trajectory^{15,16} of a single atom at the standard quantum limit.

In contrast to highly energetic charged particles, whose trajectories can be observed using ionization detectors, single neutral atoms are much harder to track. The reason is that the interaction of neutral particles with a detector is much weaker than that of charged particles. So far, the most efficient means of detecting single atoms is light scattering. However, the scattering rate is limited by the natural decay rate of the atom's excited state and the photons are emitted in random directions. Therefore, the signal becomes vanishingly small if rapid measurements must be performed, for example in the implementation of fast feedback on single atoms perturbed by quickly changing random forces.

In this context, optical cavity quantum electrodynamics provides a powerful technique for single-atom tracking and feedback owing to its unique observation^{13,14} and control capabilities^{9,17}, respectively. Measurements are faster and more sensitive than in free space, as a result of the increased rate of information exchange between the atom and the observed cavity field. This makes it possible to estimate the atomic trajectory quickly and use this position information to steer the atom rapidly in the desired direction. An advantage of such a strategy is that the steering force is automatically synchronized with the atomic motion. This is useful if the atom is moving in an anharmonic potential (as here) where the oscillation period depends on the oscillation amplitude, in which case an actuator operated at a fixed frequency is insufficient. More importantly, it makes it possible to control the atomic motion even if this motion is unpredictable on timescales as short as the oscillation period in the trap.

Unlike in previous work^{9,10}, the actuator uses blue-detuned dipole light that pushes the atom towards the area of low light intensity in the centre of the cavity¹⁷. This has three benefits, which we found to be essential. First, the dipole laser induces hardly any shift in the

energy levels of the atom, so tracking and steering are largely independent of each other. Second, the dipole laser controls the motion perpendicular to the cavity axis, which is the typical escape direction for a trapped atom. Third, it leaves the atomic motion along the cavity axis unperturbed and does not interfere with cavity cooling along this direction. As a result, we are able to study the deterministic, as well as the probabilistic, nature of the atomic trajectory by tuning the observation time interval and measuring the system response.

The system is sketched in Fig. 1. A high-finesse cavity supports a TEM₀₀ mode (waist, ~29 μm) nearly resonant with the transition

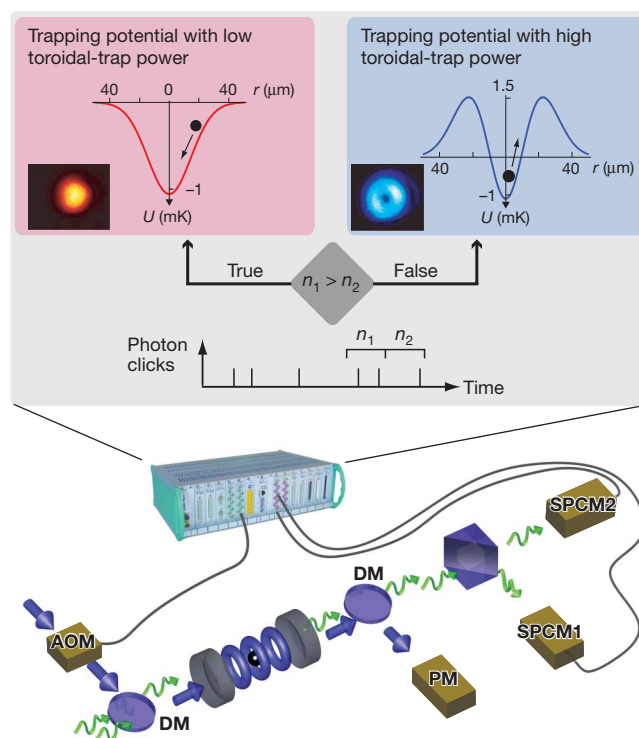


Figure 1 | Experimental setup including the feedback loop. An optical cavity directs the transmitted light to two single-photon counting modules (SPCM1, SPCM2). A real-time processor determines the sums of the photon clicks of both detectors in two consecutive time windows, n_1 and n_2 , of equal duration, T . To reduce the kinetic energy of the atom, the algorithm switches the toroidal blue-detuned dipole trap to high power if the atom attempts to leave the trap (here for $n_1 \leq n_2$) and to a low power if the atom returns towards the cavity axis ($n_1 > n_2$). The power of the toroidal trap is switched using an acousto-optical modulator (AOM), superimposed with the probe light using a dichroic mirror (DM) and detected using a photomultiplier (PM). The resulting trapping potential, U , is plotted as a function of the radial distance from the cavity centre, r , for low power (red box) and high power (blue box).

¹Max-Planck-Institut für Quantenoptik, Hans-Kopfermann-Strasse 1, D-85748 Garching, Germany.

from the $5^2S_{1/2}, F = 3, m_F = 3$ state to the $5^2P_{3/2}, F = 4, m_F = 4$ state in ^{85}Rb atoms (wavelength, 780 nm), which results in a maximum atom–cavity coupling of $g_0/2\pi = 16$ MHz, exceeding losses due to atomic polarization decay (rate, $\gamma/2\pi = 3$ MHz) and cavity field decay (rate, $\kappa/2\pi = 1.25$ MHz). A weak probe laser excites this mode at the input mirror. In addition, a red-detuned dipole-trap laser of wavelength 785 nm (not drawn) resonantly excites a second TEM₀₀ mode¹⁸, confining the atom in the cavity (trap depth, ~ 1 mK). A separate, blue-detuned, dipole trap is implemented at 775 nm and consists of a TEM₁₀ and a TEM₀₁ mode, each of which is blue-detuned with respect to the probe light by two free spectral ranges. Together they form a toroidal repulsive trap¹⁷. Because in a cylindrically symmetric system circular orbits do not modulate the transmitted light, and because cylindrically symmetric forces cannot change the angular momentum of the atomic trajectory, we break the cylindrical symmetry by making the TEM₀₁ component 50% stronger than the TEM₁₀ component. The light exiting through the output mirror is separated into probe light and trap light, and the probe light is split by a non-polarizing beam splitter and detected using two single-photon counting modules. The probe laser is almost resonant with the empty cavity (detuned by $2\pi \times 100$ kHz) and is detuned from the Stark-shifted atomic resonance by $2\pi \times 20$ MHz. For such parameter choices, a well-coupled atom will induce a drop in the transmission from 1 photon per microsecond (for an empty cavity) to typical values as low as 0.03 photons per microsecond.

Our digital feedback algorithm uses the blue toroidal trap as an ‘actuator’. The input signal is sensitive to the atomic trajectory in real time. An increase in the transmission indicates a lower coupling to the mode, as happens when an atom leaves the cavity. This information is extracted by the feedback processor (ADwin-Pro II system), which compares the respective numbers of photon clicks, n_1 and n_2 , registered during two consecutive user-defined intervals of equal duration, T , the exposure time. Differential feedback routines are used to switch the torus potential whenever a turning point of the atomic trajectory in the radial direction is registered. To achieve a high efficiency, we apply a ‘bang-bang’ strategy¹², in which the intensity of the torus potential is switched, using an acousto-optical modulator, between two extreme powers: 50 nW (low), resulting in an overall trap depth of 1 mK, and 800 nW (high), corresponding to 2.5 mK.

We implement two feedback strategies, which work as follows. In the ‘normal’ feedback strategy, we decrease the kinetic energy of the atom and keep it in the cavity centre. This is done by switching the toroidal trap to high power as soon as the atom attempts to leave the cavity, and switching it to low power as soon as the atom moves towards the cavity axis; see Fig. 1 and Fig. 2a. In the ‘inverted’ feedback strategy, the switching protocol is reversed, increasing the kinetic energy of the atom and expelling it from the cavity.

To be able to follow these strategies as closely as possible, we designed fast digital feedback logic that can react to the detection of a single photon with a decision-making time of $1.7 \mu\text{s}$ and a maximum switching-process delay of $3 \mu\text{s}$. This is much faster than the radial oscillation, which has a period of $\sim 360 \mu\text{s}$, so feedback occurs in real time. We note that the transmission signal is modulated at half the oscillation period, T_{osc} of the atom, owing to the symmetry of the cavity modes. For exposure times $T \approx T_{\text{osc}}$, the signal becomes averaged, increasing the signal-to-noise ratio but delaying the algorithm. For $T < T_{\text{osc}}$, the algorithm is fast but only partial information about the atomic trajectory is acquired. We assume that the atom leaves the cavity radially for an increasing photon flux ($n_1 < n_2$) and that the atom returns towards the cavity axis for a decreasing photon flux ($n_1 > n_2$). Both feedback strategies are shown in Fig. 2b for a short exposure time, $T = 10.2 \mu\text{s}$. Here the n_1 and n_2 values are mostly zero. Nevertheless, the normal feedback strategy keeps the photon rate low, indicating good confinement of the atom. In contrast, the inverted feedback strategy leads to an increasing photon flux. Figure 2c shows an example for a longer exposure time, $T = 85 \mu\text{s}$. Here the integrated signal becomes a smooth function, resulting in smoother switching.

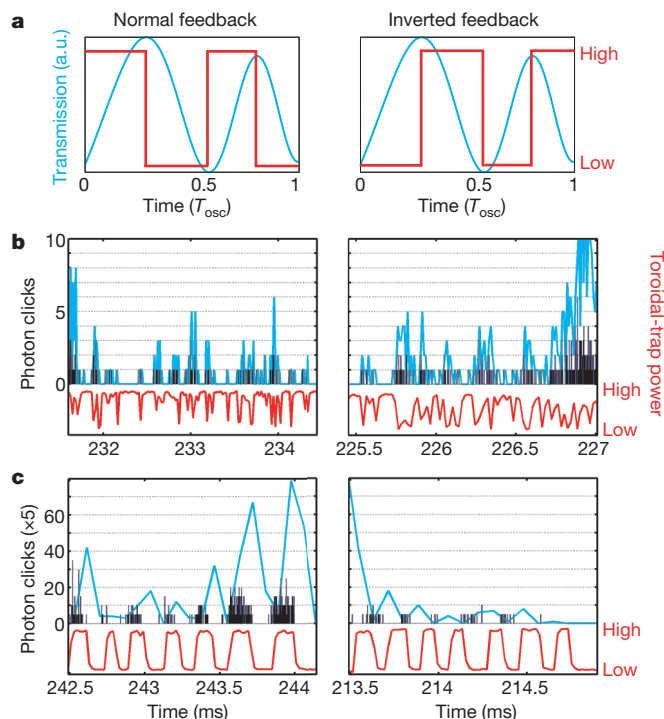


Figure 2 | Feedback protocol for a single-atom trajectory. **a**, The idealized transmission (blue) and feedback reaction (red) are displayed for an atom oscillating in the trap. For normal feedback (left column), the toroidal trap is switched to low power for decreasing cavity transmission and to high power otherwise. For inverted feedback (right column), the switching behaviour is reversed. a.u. arbitrary units. **b**, The two strategies are shown for a short exposure time, $T = 10.2 \mu\text{s}$. Single photon clicks are indicated in black and their integration over the exposure time is indicated in blue. Normal feedback keeps the atom in a well-coupled regime, reducing the oscillation amplitude, whereas inverted feedback is out of phase with the atom’s oscillation and therefore increases the oscillation amplitude to the point at which the atom leaves the trap. **c**, For a long exposure time, $T = 85 \mu\text{s}$, inverted feedback is in phase, reducing the oscillation, whereas normal feedback is not. Data for single photon clicks is shown multiplied by a factor of five, for clarity.

Concurrently, a large exposure time also delays the feedback, which can be seen by comparing the raw photon clicks (black data) with the integrated signal (blue data). For this exposure time, normal feedback is out of phase with the radial oscillation and therefore drives the atom out of the cavity. As inverted feedback is also delayed by one-quarter of an oscillation period, it turns into a damping force.

Special attention must be paid to the case in which $n_1 = n_2$. We found that the feedback is effective only if we switch the toroidal trap to low power for $n_1 > n_2$ and to high power for $n_1 \leq n_2$. A possible explanation is that for short exposure times, T , the zero-photon events are the most likely for atoms near the cavity axis. For the chosen, near-resonant, probing of the system, the photon flux depends only marginally on the exact atomic position when the coupling strength is large. Hence, if $n_1 = n_2 = 0$ the atom could already be moving away from the axis, in which case it is prudent to switch the toroidal trap to high power.

To analyse the performance of our feedback strategies quantitatively, we study the atomic storage time, which is mainly determined by radial losses of the atom for the chosen parameters. The storage time is obtained by fitting an exponential decay to the atomic storage probability. The first millisecond is dominated by a rapid loss of atoms, presumably those that are not injected in one of the central antinodes. Therefore, the first millisecond of data is disregarded (fraction of remaining atoms, $\sim 55\%$).

Figure 3 shows the atomic storage probability as a function of time (plotted in the inset) and the average storage time as a function of

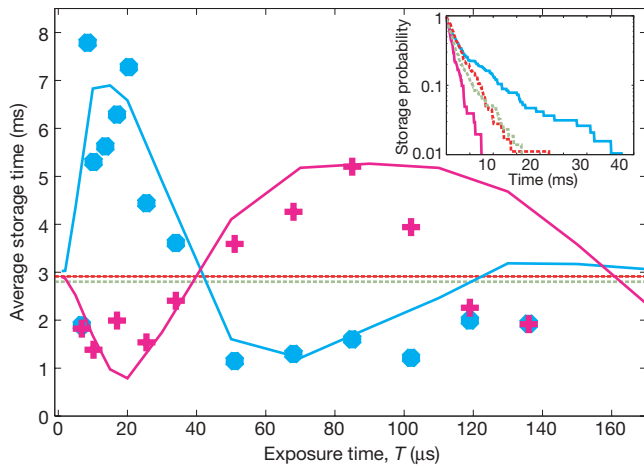


Figure 3 | Manoeuvring of a single atom using real-time feedback. Average storage time plotted as a function of exposure time for two feedback strategies. The solid lines show the results of Monte Carlo simulations for the inverted (magenta) and normal (blue) feedback strategies. The corresponding experimental data points are plotted in the same colours. The dotted green and red lines show the experimental storage times without feedback for high and, respectively, low toroidal-trap power, setting the boundary between feedback cooling (longer storage time) and feedback heating (shorter storage time). The standard deviations (not shown) obtained from exponential fits to the decay (see text) are less than 0.18 ms. The inset shows the experimental atom-loss dynamics without feedback (green and red dashed lines, colour-coded as in main figure) and illustrates how the feedback changes the slope of the exponential decay. Whereas the slope is less steep for normal feedback ($T = 17 \mu\text{s}$; blue), it is more steep for inverted feedback ($T = 25.5 \mu\text{s}$; magenta).

exposure time, T , ranging from a few microseconds to $T \approx 140 \mu\text{s}$ or, in other words, from a small fraction of the oscillation period to about three-eighths of it. The dotted red and green lines are the storage times with the toroidal trap at low and, respectively, high power without feedback. When T is less than $\sim 7 \mu\text{s}$, the noise dominates the signal and the algorithm mainly reacts to the random arrival of photons. This results in a heating of the atom and a decrease in the storage time to below the zero-feedback value, for both normal (blue points) and the inverted (magenta points) feedback. Increasing the exposure time, however, increases the storage time, with a maximum at $T \approx 15 \mu\text{s}$ for normal feedback. This is remarkable, given that only a few photons have been detected. In contrast, applying inverted feedback at this value of T leads to a storage time less than the value obtained without feedback. Here we are heating the atom by acting out of phase with its motion. Furthermore, we see that inverted feedback turns into a cooling mechanism for longer exposure times, reaching a maximum at $T \approx 90 \mu\text{s}$. The maximum storage time for inverted feedback is less than that obtained for normal feedback. This directly shows that it is important to apply the feedback before the atomic motion becomes unpredictable.

To understand the data better, we performed Monte Carlo simulations of the experiment. As shown by the solid lines in Fig. 3, there is good agreement between the simulations and the measurements. The storage times are well reproduced if we add a loss mechanism other than cavity-induced heating. The main reason for this loss is the possibility of off-resonant pumping of the atom into the ‘dark’ hyperfine state, in which $F = 2$ (ref. 19). We analysed this effect by adding a repumper laser perpendicular to the cavity axis. From the increase in the storage time without feedback, we can estimate the additional loss rate to be between $1/5.5 \text{ ms}^{-1}$ and $1/14 \text{ ms}^{-1}$. Including a rate of $1/7 \text{ ms}^{-1}$ in the simulation shows good agreement with the experimental data. We also found experimentally that the storage time with feedback increases to $\sim 15 \text{ ms}$ when the repumper laser is added.

We next analyse the atomic motion by imposing limits on the average transmitted power (and, thus, on the average atom–cavity

coupling strength) in the data evaluation²⁰. Photon correlations now reveal further information on the dynamics of atomic motion, as shown in Fig. 4. Here photon bunching is caused by fluctuations in the coupling strength. For measurements with a weak atom–cavity coupling, corresponding to a transmission of up to 0.6 times that of the empty cavity, the oscillation period is $\sim 2 \times 260 \mu\text{s}$ (dashed line). If the transmission is restricted to be less than 0.05 times that of the empty cavity, the oscillation period decreases to $\sim 2 \times 180 \mu\text{s}$ (solid line). Comparison with Fig. 3 therefore shows that the maximum in the average storage time at $\sim 90 \mu\text{s}$ corresponds to one-quarter of the oscillation period for a well-coupled atom. A further comparison with simulations shows that the feedback can keep the atom close to the cavity axis, with an average excursion of less than $4.5 \mu\text{m}$. This is a factor of ~ 2 less than the value obtained without feedback. We note that the crossing from in-phase behaviour to out-of-phase behaviour occurs for $T \approx 45 \mu\text{s}$ (Fig. 3), which is one-eighth of the oscillation period for a well-coupled atom. In addition, the random character of the atomic motion is visible in the damping of the correlation function, indicating a decoherence time of $\sim 200 \mu\text{s}$. The dependence of the oscillation period on the localization is shown in the inset of Fig. 4. It shows the anharmonicity of the atomic motion; a harmonic potential would result in a horizontal line.

Further improvement of the feedback algorithm is possible and has already been realized by combining a fast reaction time with smooth switching behaviour: a fast loop with a short exposure time, $T_{\text{short}} = 8.5 \mu\text{s}$, is responsible for switching the toroidal trap to low power whenever the atom is observed to move towards the cavity axis ($n_1 > n_2$). Proper switching of the trap back to high power when the atom is close to the cavity axis is more critical, as here the photon flux from the cavity is low. To improve the signal-to-noise ratio, we added a loop with a longer exposure time, $T_{\text{long}} = 34 \mu\text{s}$, corresponding to about $T_{\text{osc}}/8$. The trap is switched back to high power only if both loops register $n_1 \leq n_2$. Using this improved algorithm, we increased the average storage time to about 24 ms, with maximum observed trapping times exceeding 250 ms. With the repumper laser on, the overall improvement factor of the storage time with feedback (24 ms) relative to that without feedback ($\leq 6 \text{ ms}$) is larger than four. Our simulations indicate that storage times of 0.5 s can be realized when spurious photon clicks (in our experiment mainly stemming from repumper light scattered from the edges of the cavity mirrors) are

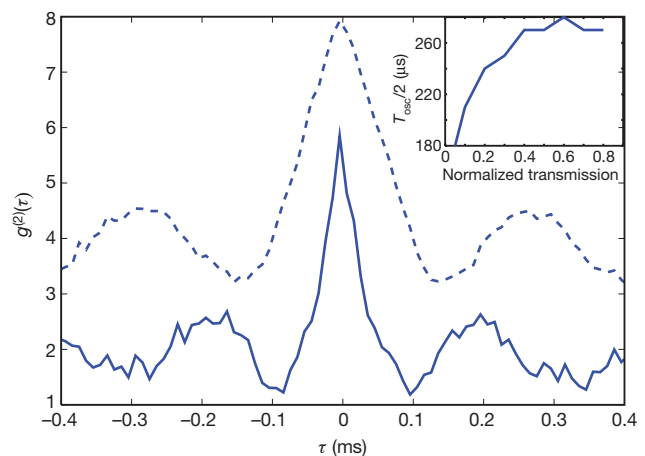


Figure 4 | Dynamics of atomic motion from photon correlation measurements. The photon correlation function, $g^{(2)}(\tau)$, is shown as function of the correlation time, τ , for strongly coupled atoms (solid line) and loosely coupled atoms (dashed line). The atomic motion leaves its signature in the correlations, allowing the determination of the oscillation period as well as the decoherence time of the oscillation, $\sim 200 \mu\text{s}$. The standard deviations (not shown) of the $g^{(2)}(\tau)$ data are typically less than 0.15. The inset shows the dependence of the oscillation period on the transmission normalized using the empty-cavity transmission, characterizing the anharmonicity of the trapping potential.

eliminated. This would make the feedback scheme compatible with state-of-the-art laser cooling techniques, but with the advantage that one-dimensional optical access is sufficient for three-dimensional control.

The successful realization of feedback on an a-priori unpredictable atomic trajectory shows that reliable position information can be obtained from continuous (or quasi-continuous) measurements. Once extended into the quantum domain, this might make it possible to stabilize the quantum state of a trapped particle or observe the quantum Zeno effect for a free particle²¹. Additional feedback might then make it possible to steer an individual quantum trajectory with a precision ultimately determined by Heisenberg's uncertainty relation.

Received 17 August; accepted 7 October 2009.

- Shapiro, J. H., Saplakoglu, G., Ho, S.-T., Kumar, P. & Saleh, B. E. A. Theory of light detection in the presence of feedback. *J. Opt. Soc. Am. B* **4**, 1604–1620 (1987).
- Wiseman, H. M. Quantum theory of continuous feedback. *Phys. Rev. A* **49**, 2133–2150 (1994).
- Jacobs, K. How to project qubits faster using quantum feedback. *Phys. Rev. A* **67**, 030301 (2003).
- Combes, J., Wiseman, H. M. & Jacobs, K. Rapid measurement of quantum systems using feedback control. *Phys. Rev. Lett.* **100**, 160503 (2008).
- Viola, L., Knill, E. & Lloyd, S. Dynamical decoupling of open quantum systems. *Phys. Rev. Lett.* **82**, 2417–2421 (1999).
- Viola, L. Advances in decoherence control. *J. Mod. Opt.* **51**, 2357–2367 (2004).
- Ashkin, A. & Dziedzic, J. M. Feedback stabilization of optically levitated particles. *Appl. Phys. Lett.* **30**, 202–204 (1977).
- Morrow, N. V., Dutta, S. K. & Raithe, G. Feedback control of atomic motion in an optical lattice. *Phys. Rev. Lett.* **88**, 093003 (2002).
- Fischer, T., Maunz, P., Pinkse, P. W. H., Puppe, T. & Rempe, G. Feedback on the motion of a single atom in an optical cavity. *Phys. Rev. Lett.* **88**, 163002 (2002).
- Lynn, T. W., Birnbaum, K. & Kimble, H. J. Strategies for real-time position control of a single atom in cavity QED. *J. Opt. B* **7**, 215–225 (2005).
- Bushev, P. *et al.* Feedback cooling of a single trapped ion. *Phys. Rev. Lett.* **96**, 043003 (2006).
- Steck, D. A., Jacobs, K., Mabuchi, H., Habib, S. & Bhattacharya, T. Feedback cooling of atomic motion in cavity QED. *Phys. Rev. A* **74**, 012322 (2006).
- Pinkse, P. W. H., Fischer, T., Maunz, P. & Rempe, G. Trapping an atom with single photons. *Nature* **404**, 365–368 (2000).
- Hood, C. J., Lynn, T. W., Doherty, A. C., Parkins, A. S. & Kimble, H. J. The atom-cavity microscope: single atoms bound in orbit by single photons. *Science* **287**, 1447–1453 (2000).
- Molmer, K., Castin, Y. & Dalibard, J. Monte Carlo wave-function method in quantum optics. *J. Opt. Soc. Am. B* **10**, 524–538 (1993).
- Carmichael, H. (ed.) *An Open Systems Approach to Quantum Optics* (Springer, 1993).
- Puppe, T. *et al.* Trapping and observing single atoms in a blue-detuned intracavity dipole trap. *Phys. Rev. Lett.* **99**, 013002 (2007).
- Maunz, P. *et al.* Cavity cooling of a single atom. *Nature* **428**, 50–52 (2004).
- Khudaverdyan, M. *et al.* Quantum jumps and spin dynamics of interacting atoms in a strongly coupled atom-cavity system. *Phys. Rev. Lett.* **103**, 123006 (2009).
- Kubanek, A. *et al.* Two-photon gateway in one-atom cavity quantum electrodynamics. *Phys. Rev. Lett.* **101**, 203602 (2008).
- Braginsky, V. B. & Khalili, F. Y. (eds) *Quantum Measurement* (Cambridge Univ. Press, 1992).

Acknowledgements Partial support by the Bavarian PhD programme of excellence QCCC, the Deutsche Forschungsgemeinschaft research unit 635 and the European Union project SCALA are gratefully acknowledged.

Author Contributions All authors contributed to the design and implementation of the experiment, the interpretation of the results and the writing of the manuscript.

Author Information Reprints and permissions information is available at www.nature.com/reprints. Correspondence and requests for materials should be addressed to A.K. (alexander.kubanek@mpq.mpg.de) or G.R. (gerhard.rempe@mpq.mpg.de).